

# Recent Developments in Non-Fermi Liquid Theory

Sung-Sik Lee

<sup>1</sup>Department of Physics & Astronomy, McMaster University,  
1280 Main St. W., Hamilton ON L8S 4M1, Canada

<sup>2</sup>Perimeter Institute for Theoretical Physics,  
31 Caroline St. N., Waterloo ON N2L 2Y5, Canada

(Dated: March 24, 2017)

## Abstract

Non-Fermi liquids arise when metals are subject to singular interactions mediated by soft collective modes. In the absence of well-defined quasiparticle, universal physics of non-Fermi liquids is captured by interacting field theories which replace Landau Fermi liquid theory. In this review, we discuss two approaches that have been recently developed for non-Fermi liquid theory with emphasis on two space dimensions. The first is a perturbative scheme based on a dimensional regularization, which achieves a controlled access to the low-energy physics by tuning the number of co-dimensions of Fermi surface. The second is a non-perturbative approach which treats the interaction ahead of the kinetic term through a non-Gaussian scaling called interaction-driven scaling. Examples of strongly coupled non-Fermi liquids amenable to exact treatments through the interaction-driven scaling are discussed.

## I. INTRODUCTION

Metal is among the most delicate states of quantum matter. Due to the presence of extensive gapless modes that support long-range entanglement in real space, metals are highly susceptible to external perturbations. In view of this, it is rather remarkable that Fermi liquid metals are more or less immune to quantum fluctuations generated by the screened Coulomb interaction. In Fermi liquids, many-body eigenstates of interacting fermions are still labeled by the occupation numbers of quasiparticles[1]. The existence of well defined single-particle excitations is attributed to the Pauli exclusion principle that severely limits non-forward scatterings near the Fermi surface[2, 3].

With the discovery of high-temperature superconductors, heavy fermion compounds and iron pnictides, it became clear that quantum criticalities provide natural routes to non-Fermi liquids which lie beyond the quasiparticle paradigm. At quantum critical points, non-Fermi liquids are realized as soft order parameter fluctuations mediate singular interactions between electrons[4–7]. Although one generally needs a fine tuning to reach a critical point in the zero temperature limit, the underlying non-Fermi liquid state can dictate the universal scaling behaviors[8] over an extended region of the phase diagram at finite temperatures. If a collective mode is protected dynamically not by a fine-tuning, non-Fermi liquid states can be realized as a phase without a fine tuning.

Arguably, non-Fermi liquids in layered systems are most interesting from theoretical perspective. Typically being below the upper critical dimension, non-Fermi liquids in two dimensions are expected to deviate strongly from the Fermi liquids. On the other hand, metals in two dimensions can support an extended Fermi surface unlike in one dimension. The combination of strong infrared quantum fluctuations and the presence of extended manifolds of gapless modes makes non-Fermi liquids in two dimensions rather unique[9–23]. Besides dimensionality, another important factor that determines universal properties of non-Fermi liquids is the wavevector,  $\vec{Q}$  carried by the soft collective mode at zero energy. For  $\vec{Q} = 0$ , low-energy collective modes induce small-angle scatterings everywhere on the Fermi surface. Examples include the nematic critical point and the U(1) spin liquid with spinon Fermi surface. In this case, the low-energy theory describes a ‘hot Fermi surface’. Non-Fermi liquids with nonzero  $\vec{Q}$  can arise near quantum critical points associated with density wave transitions of spin, charge or orbital. With  $\vec{Q} \neq 0$ , fermions can interact with low-energy collective modes only near a sub-manifold of the Fermi surface connected by  $\vec{Q}$ . In two dimensions, the sub-manifold is a discrete set of ‘hot spots’.

The first part of the review covers non-Fermi liquids with hot Fermi surfaces. In Sec. II A, we introduce the theory that describes the non-Fermi liquid realized at the Ising-nematic quantum critical point in two dimensions. Among the schemes that have been proposed for the purpose of gaining a controlled access to the physics of non-Fermi liquid, we focus on a dimensional regularization scheme which tunes the number of co-dimensions of Fermi surface. Although the dimensional regularization scheme allows one to understand non-Fermi liquids reliably near the upper critical dimension, the perturbative approach has the fundamental limit when applied to the strongly coupled theory in two dimensions. In Sec. II B, a non-perturbative approach which treats interactions ahead of the kinetic term is discussed. In particular, we introduce the notion of interaction-driven scaling, and discuss an example of non-Fermi liquids whose exact critical exponents can be obtained from the interaction-driven scaling. The second half of the review covers the antiferromagnetic quantum critical metal as an example of hot-spot theories. In Sec. III A, the perturbative results obtained from the dimensional regularization scheme are discussed. In Sec. III B, we discuss the non-perturbative solution for the theory in two dimensions, which gives exact critical exponents through an Ansatz constructed from the interaction-driven scaling.

## II. THEORY OF HOT FERMI SURFACE

The Ising-nematic phase transition refers to a spontaneous breaking of the four-fold rotational symmetry to the two-fold symmetry. A positive or negative order parameter represents one of the two symmetry breaking patterns. If a metal undergoes a nematic quantum phase transition, a non-Fermi liquid arises at the critical point[18, 21, 24–29]. The Ising order parameter is strongly damped by particle-hole excitations while fermions near the Fermi surface undergo persistent scatterings by the fluctuating order parameter. The theoretical goal is to capture the universal properties that result from the interplay between the gapless collective mode and soft fluctuations of the Fermi surface.

In two dimensions, the nematic order parameter is coupled to the quadrupolar distortion of the Fermi surface,  $H_{int} = \sum_{\vec{K}, \vec{q}} (\cos K_x - \cos K_y) \phi(\vec{q}) c_j^\dagger(\vec{K} + \vec{q}) c_j(\vec{K})$ , where  $\phi(\vec{q})$  is the collective mode for the nematic order parameter with momentum  $\vec{q}$ , and  $c_j(\vec{K})$  is the electron field with momentum  $\vec{K}$  and spin  $j = \uparrow, \downarrow$ . The fermion at momentum  $\vec{K}$  on the Fermi surface is mainly coupled with the collective mode whose momentum is tangential to the Fermi surface at  $\vec{K}$ . This is because fermions can absorb or emit bosons whose momenta are tangential to the Fermi sur-

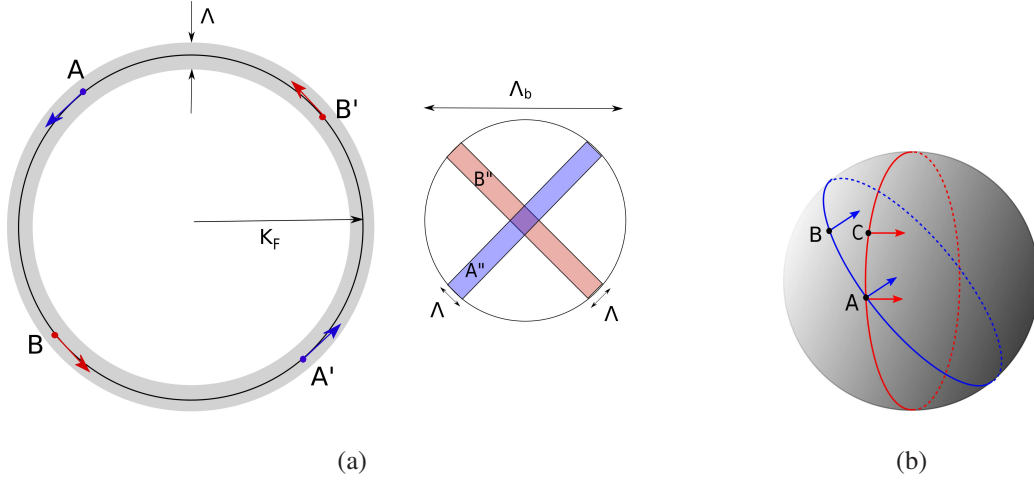


FIG. 1: (a) The origin of the emergent locality in momentum space. The left figure represents a Fermi surface with size  $K_F$ . The shaded region is the phase space for low-energy fermionic excitations with an energy cut-off  $\Lambda \ll K_F$ . The right figure denotes the momentum space of a collective mode. The momentum cut-off for the collective mode  $\Lambda_b \sim \sqrt{K_F \Lambda}$  is much larger than  $\Lambda$  because a fermion can absorb a boson with momentum much larger than  $\Lambda$  if the momentum of the boson is parallel to the Fermi surface. When Fermi surface is one-dimensional, there exists only a discrete set of points whose tangent vectors are parallel or anti-parallel to each other. For example, point  $A$  ( $B$ ) share the anti-parallel tangent vector only with point  $A'$  ( $B'$ ). Therefore the fermions near  $A$  and  $A'$  ( $B$  and  $B'$ ) couple only with the boson in region  $A''$  ( $B''$ ) at low energies. Since the overlap between  $A''$  and  $B''$  becomes vanishingly small in the low energy limit, the sector that describes  $\{A, A', A''\}$  decouples from that of  $\{B, B', B''\}$ . (b) The locality in momentum space is lost as soon as the dimension of Fermi surface becomes greater than one. When the dimension of Fermi surface is greater than one with co-dimension one, one can find a common tangent vector for any two points on the Fermi surface. For example, the point  $A$  have tangent vectors that are tangent to point  $B$  and  $C$  on a two-dimensional Fermi surface.

face while staying close to the Fermi surface. Because fermions from different patches of Fermi surface interact with the boson with largely disjoint sets of momenta, the inter-patch coupling is small in the low energy limit, unless the Fermi surfaces in two patches are locally parallel or anti-parallel[14, 30]. This is illustrated in Fig. 1(a). The exception that breaks the locality in momentum space is the short-range four-fermion interaction in the pairing channel. We will discuss the issue of superconductivity at the end of the section.

The locality in momentum space allows one to decompose the full theory into a sum of two-

patch theories. Each two-patch theory describes electronic excitations near two antipodal points and the collective mode whose momentum is close to be tangential to the Fermi surface at the antipodal points. Let us consider the two-patch theory which describes the patches centered at  $\vec{K} = \pm K_F \hat{x}$ . The action is written as

$$\begin{aligned}
S = & \sum_{s=\pm} \sum_{j=\uparrow,\downarrow} \int \frac{d^3k}{(2\pi)^3} \psi_{s,j}^\dagger(k) \left[ ik_0 + sk_x + k_y^2 \right] \psi_{s,j}(k) \\
& + \frac{1}{2} \int \frac{d^3q}{(2\pi)^3} \left[ q_0^2 + c_x^2 q_x^2 + c_y^2 q_y^2 \right] |\phi(q)|^2 \\
& + g_0 \sum_{s=\pm} \sum_{j=\uparrow,\downarrow} \int \frac{d^3k d^3q}{(2\pi)^6} \phi(q) \psi_{s,j}^\dagger(k+q) \psi_{s,j}(k). \tag{1}
\end{aligned}$$

Here  $k = (k_0, k_x, k_y)$  denotes the frequency and momentum in the Euclidean spacetime.  $\psi_{+,j}(k) = c_j(k_0, K_F \hat{x} + \vec{k})$  and  $\psi_{-,j}(k) = c_j(k_0, -K_F \hat{x} + \vec{k})$  represent the right and left moving fermion with spin  $j$  respectively. The momentum for the fermion field has been shifted such that  $\vec{k} = 0$  represents the point on the Fermi surface in each patch.  $k_x, k_y$  have been rescaled independently so that the absolute value of Fermi velocity and the local curvature of the Fermi surface become one.  $g_0$  is the fermion-boson coupling, and  $(c_x, c_y)$  is the velocity of the collective mode. Theories for other types of non-Fermi liquids with hot Fermi surface are similar to Eq. (1). The only major modification is the nature of the vertex in the coupling. One exception is when the Fermi surface is not locally parabolic[22]. For example, non-parabolic patches arise near inflection points on Fermi surface, which can be viewed as a ‘multi-critical’ theory tuned by the angle around the Fermi surface.

One of the most important aspects of metal is the fact that there are infinitely many gapless modes near the Fermi surface. One way to formalize this is to view the Fermi surface in two dimensions as an infinite set of one-dimensional Dirac fermions, where the momentum along the Fermi surface labels the continuously many gapless modes. To make this precise, the right and left moving fermions can be combined into a spinor,  $\Psi_j(k)^T = (\psi_{+,j}(k), \psi_{-,j}^\dagger(-k))$ . In this representation, the fermion kinetic term becomes  $S_F = \sum_j \int \frac{d^3k}{(2\pi)^3} \bar{\Psi}_j(k) \left[ ik_0 \gamma_0 + i(k_x + k_y^2) \gamma_1 \right] \Psi_j(k)$ , where  $\gamma_0 = \sigma_y, \gamma_1 = \sigma_x$  are the gamma matrices for the two component spinor, and  $\bar{\Psi} \equiv \Psi^\dagger \gamma_0$ . Because the Fermi surface is locally parabolic, the scaling dimension of  $k_y$  is half the dimension of  $k_x$ . Under the tree-level scaling that leaves the kinetic terms invariant, only  $q_y^2 |\phi(q)|^2$  is marginal for the boson kinetic term, and  $(q_0^2 + c_x^2 q_x^2) |\phi(q)|^2$  can be dropped. Physically, this implies that the dynamics of the boson is strongly dressed by particle-hole excitations to the extent

that some parts of the bare kinetic term become unimportant at low energies.

### A. Perturbative approach

At the non-interacting fixed point, the coupling has the scaling dimension  $1/2$ , and grows as energy is lowered. Given that there is no general non-perturbative method for strongly coupled theories, it is natural to start by deforming the theory so that the effect of quantum fluctuations can be included perturbatively.

Over the years, different theoretical schemes have been proposed to this end. The most straightforward deformation is to enlarge the number of spin components to a large number  $j = 1, 2, \dots, N$ [11, 12, 14]. In relativistic quantum field theories, the mean-field theory is applicable in the large  $N$  limit, and quantum fluctuations can be perturbatively included order by order in the  $1/N$  expansion. However, this is no longer the case in the presence of Fermi surface. Due to the abundance of soft particle-hole excitation near the Fermi surface, low-energy quantum fluctuations are not completely tamed even in the large  $N$  limit. The angle around the Fermi surface effectively becomes an additional flavor, which turns the theory to be like a matrix theory. The resulting theory is not solvable even in the large  $N$  limit due to the proliferation of planar graphs[17]. In the one-patch theory that describes non-Fermi liquids without time-reversal and parity invariance, the  $1/N$  expansion is organized by the genus of Feynman diagrams. For non-chiral theories, even non-planar diagrams play an important role[18]. Understanding the nature of non-Fermi liquids in the large  $N$  limit remains as an open problem. As alternatives, the limits in which the number of fermionic species is much smaller than the number of bosonic species have been also considered[11, 31, 32].

Another deformation scheme is a dynamical tuning, where one tunes the bare dispersion of excitations[16, 19]. For example, one can change the kinetic term of the collective mode to  $|\vec{q}|^{1+\epsilon}|\phi(q)|^2$ , where  $\epsilon$  is a tuning parameter. As  $\epsilon$  decreases from 1, the density of state for the collective mode is reduced at low energies, and one can use  $\epsilon$  as a control parameter to tame quantum fluctuations. This scheme has the merit of keeping a finite density of state of fermion and preserving all microscopic symmetries. A downside is that it breaks the locality in real space, which blocks the collective mode from acquiring an anomalous dimension.

Finally, dimensional regularization schemes are considered. Unlike relativistic field theories, both the space dimension  $d$  and the dimension of Fermi surface  $d_f$  can be tuned independently[33].

Among the infinitely many ways to approach the original theory with  $(d, d_f) = (2, 1)$ , the most intuitive extension is probably to keep the co-dimension  $(d - d_f)$  of the Fermi surface fixed[34, 35]. Under such an extension, the fermion kinetic term is generalized to  $S_F = \sum_j \int \frac{d^{d+1}k}{(2\pi)^{d+1}} \bar{\Psi}_j(k) \left[ ik_0 \gamma_0 + i(k_1 + \sum_{\mu=2}^d k_\mu^2) \gamma_1 \right] \Psi_j(k)$  in  $d$  space dimensions. While this has the advantage of keeping a non-zero density of states at zero energy, it has a drawback of spoiling the emergent locality in momentum space (not in real space). For  $d_f > 1$ , any two points on the Fermi surface share a common tangential vector as is illustrated in Fig. 1(b), and fermions remain strongly coupled across the entire Fermi surface. Since the size of Fermi surface enters as a relevant scale in all low energy observables, a UV/IR mixing arises[33].

The dimensional regularization scheme that avoids the UV/IR mixing is the one in which the manifold of the gapless modes is unchanged as the number of dimensions is tuned [21, 36, 37]. Although it seems unnatural, the deformation which tunes the number of co-dimensions is in line with the original idea of dimensional regularization scheme applied to relativistic quantum field theories, where the number of gapless points in momentum space is not increased while the space dimension is increased. One takes advantage of the reduced densities of state to control quantum fluctuations at low energies. More concretely, one extends the theory in two dimensions to a theory that describes a line node in general dimensions whose kinetic energy reads  $S_F = i \sum_j \int \frac{d^{d+1}k}{(2\pi)^{d+1}} \bar{\Psi}_j(k) \left[ \sum_{\mu=0}^{d-2} k_\mu \gamma_\mu + (k_{d-1} + k_d^2) \gamma_2 \right] \Psi_j(k)$ , where  $k_1, \dots, k_{d-2}$  are the newly added directions which are transverse to the Fermi surface, and  $(k_{d-1}, k_d)$  represents the original two-dimensional plane in which the line node is located. In three dimensions, the theory describes a  $p$ -wave superconductor with a line node. This scheme has the advantage of keeping the locality in real space and the emergent locality in momentum space. The drawback of this scheme is to break certain symmetry of the original model in gapping out the parts of the Fermi surface away from the line nodes. In this case, the global  $U(1)$  associated with the transformation  $\Psi \rightarrow e^{i\theta\sigma_3} \Psi$  is broken down to  $Z_2$  by pairing. While the full symmetry can be kept if one gives up locality in real space[36], one has to pay the price of breaking some symmetry if one keeps the locality in real space[21, 37].

Among the deformation schemes discussed above, we employ the latter dimensional regularization scheme which puts more emphasis on localities (both in real and momentum spaces) than symmetry. The theory that continuously interpolates the Fermi surface in two dimensions to the

line node in three dimensions reads[21]

$$\begin{aligned}
S = & \sum_j \int \frac{d^{d+1}k}{(2\pi)^{d+1}} \bar{\Psi}_j(k) \left[ i\boldsymbol{\Gamma} \cdot \mathbf{K} + i\gamma_{d-1}\delta_k \right] \Psi_j(k) + \frac{1}{2} \int \frac{d^{d+1}q}{(2\pi)^{d+1}} q_y^2 \phi(-q)\phi(q) \\
& + \frac{i\sqrt{d-1}}{\sqrt{N}} g\mu^{\frac{5-2d}{4}} \sum_j \int \frac{d^{d+1}k d^{d+1}q}{(2\pi)^{2d+2}} \phi(q) \bar{\Psi}_j(k+q) \gamma_{d-1} \Psi_j(k). \tag{2}
\end{aligned}$$

Here the spin index is generalized to  $j = 1, 2, \dots, N$ .  $\mathbf{K} \equiv (k_0, k_1, \dots, k_{d-2})$  represents frequency and  $(d-2)$  components of the full  $(d+1)$ -dimensional energy-momentum vector.  $\delta_k = k_x + \sqrt{d-1}k_y^2$  is the energy dispersion of the fermion in the two-dimensional subspace, where we keep the notation  $k_x, k_y$  in favor of  $k_{d-1}, k_d$ . The gamma matrices associated with  $\mathbf{K}$  are written as  $\boldsymbol{\Gamma} \equiv (\gamma_0, \gamma_1, \dots, \gamma_{d-2})$ . Since the space dimension of interest lies between 2 and 3, the number of spinor components is fixed to be two. The Fermi surface is located at  $k_1 = \dots = k_{d-2} = 0$  and  $\delta_k = 0$ . The  $(d-1)$  constraints for  $d$  components of momentum gives a one-dimensional manifold embedded in the  $d$ -dimensional momentum space. In Eq. (2),  $c_y$  has been absorbed into the field redefinition.  $\mu$  is an energy scale introduced to make  $g$  dimensionless. The upper critical dimension of the theory is  $d_c = 5/2$ , and the non-Fermi liquid state can be accessed perturbatively in  $d = 5/2 - \epsilon$  for small  $\epsilon$ .

In computing the quantum effective action that determines physical observables, there is one peculiar feature that is not present in relativistic field theories. Because the minimal action does not include the full kinetic term for the collective mode, the boson propagator needs to be dressed with self-energy before loops that include internal boson lines are computed. At the one-loop order, the boson propagator becomes

$$D_1(k) = \frac{1}{k_y^2 + \beta_d g^2 \mu^\epsilon \frac{|\mathbf{K}|^{d-1}}{|k_y|}}, \tag{3}$$

where  $\beta_d$  is a constant that is finite in  $2 \leq d < 3$ . For other one-loop diagrams, say the one-loop fermion self-energy, one should use Eq. (3) for the internal boson propagator. Since the boson propagator itself depends on the coupling  $g$ , the one-loop fermion self-energy becomes order of  $g^{4/3}$  instead of  $g^2$ . The non-analyticity in the coupling is a sign that some quantum effects for the boson self-energy are included non-perturbatively. At the next order, one includes not only the two-loop fermion self-energy computed with the one-loop dressed boson propagator, but also the correction generated from updating the boson propagator inside the one-loop fermion self-energy graph with the two-loop boson self-energy. This unusual order of including Feynman diagrams is forced upon us by the dynamical structure of the theory. Although the expansion is not organized

by the number of loops, the procedure guarantees that every Feynman diagram is included once and only once order by order in  $\epsilon$ .

Requiring that the physical observables are finite for  $0 \leq \epsilon \leq 1/2$ , we add local counter terms that remove poles in  $1/\epsilon$ . The bare theory that generates finite physical observables is given by the sum of the classical action and the counter terms. From the condition that the bare theory is independent of the scale at which the low-energy observables are defined, one obtains the beta function that describes the flow of the renormalized coupling as a function of scale. To the order of  $O(\epsilon^2)$ , the beta function becomes

$$\frac{dg}{dl} = \frac{\epsilon}{2}g - 0.02920 \left( \frac{3}{2} - \epsilon \right) \frac{g^{7/3}}{N} + 0.01073 \left( \frac{3}{2} - \epsilon \right) \frac{g^{11/3}}{N^2}, \quad (4)$$

where  $l$  is the logarithmic length scale. It exhibits a stable interacting fixed point at  $\frac{g^{*4/3}}{N} = 11.417\epsilon + 55.498\epsilon^2$ . Because the two-point functions are insensitive to the size of the Fermi surface, the propagators obey the scaling forms,

$$D(k) = \frac{1}{k_y^{2(1-\tilde{\eta}_\phi)}} f \left( \frac{|\mathbf{K}|^{1/z}}{k_y^2} \right), \quad G(k) = \frac{1}{|\delta_k|^{1-\tilde{\eta}_\psi}} g \left( \frac{|\mathbf{K}|^{1/z}}{\delta_k} \right). \quad (5)$$

Here the dynamical critical exponent is related to the anomalous dimension of the boson through  $z = \frac{3-2\tilde{\eta}_\phi}{3-2\epsilon}$ . The exact relation is due to the Ward identity which originates from the fact that the boson couples to the  $(d-1)$ -th component of a conserved current associated with the unbroken  $U(1)$  symmetry,  $\Psi \rightarrow e^{i\varphi}\Psi$ [18, 19, 21]. To the two-loop order, the anomalous dimensions are given by  $\tilde{\eta}_\phi = 0$ ,  $\tilde{\eta}_\psi = 0.1508\epsilon^2$ . It happens that the anomalous dimension of boson remains zero, and  $z = \frac{3}{2}$  in two dimensions up to the three-loop order. This is due to the facts that  $\tilde{\eta}_\phi = 0$  is exact for the single-patch theory[22], and the presence of the antipodal points in the two-patch theory does not play an important role up to the three-loop order[21]. However, there is no symmetry that protects the scaling dimension of the boson, and a non-trivial anomalous dimension, which causes a deviation of  $z$  from  $3/2$ , is expected to arise at higher loops[23].

Unlike the correlation functions that are local in momentum space, thermodynamic responses and transport properties are sensitive to the size of the Fermi surface. As low-energy excitation across the entire Fermi surface contribute to the thermodynamic responses and transport, they violate the hyperscaling[21, 38]. Due to the emergent locality in momentum, the free energy is linearly proportional to the size of Fermi surface which provides a cut-off for  $k_y$ . Since the specific heat has dimension  $[c_V] = z(d-2) + \frac{3}{2}$ , it scales with temperature as  $c_V \sim \Lambda_y T^{(d-2)+\frac{1}{z}}$ , where  $\Lambda_y$

is a scale associated with the size of Fermi surface which accounts for the violation of hyperscaling by dimension  $[k_y] = 1/2$ .

Under the tree-level patch scaling, a short-range four-fermion interaction has the scaling dimension  $(3/2 - d)$ . Although it is irrelevant by power counting in two dimensions and above, this itself does not exclude perturbative superconducting instability for the following reasons. First, the pairing susceptibility does not obey hyperscaling because all fermions near Fermi surface contribute to pairing with zero center of mass momentum. The violation of hyperscaling enhances the effective scaling dimension of the four-fermion interaction to  $(2 - d)$  through the scale  $\Lambda_y$  [33]. Second, the soft collective mode feeds the four fermion coupling in the pairing channel with small momentum transfer[39–41]. While the non-Fermi liquid remains stable against pairing near  $d = 5/2$ , the density of state increases, and the pairing interaction becomes stronger as  $d = 2$  is approached. As a result, the system becomes unstable against pairing below a certain critical dimension which lies between 2 and  $5/2$ [40, 42–44].

## B. Non-perturbative approach

Although the perturbative approach discussed in the previous section provides some insight into non-Fermi liquids, the strongly interacting theory in two dimensions is far from being understood in general. One of the exceptions is a chiral non-Fermi liquid, where exact critical exponents can be extracted.

A chiral metal can arise on the surface of three-dimensional topological states. For example, the surface of a stack of  $\nu = 1$  quantum Hall layers supports a two-dimensional metallic state as the chiral edge modes acquire dispersion in the direction perpendicular to the layers through inter-layer tunnelings[45]. The kinetic term for the chiral Fermi surface can be written as

$$H_F = \sum_K (K_x - t \cos(K_y)) c_j^\dagger(\vec{K}) c_j(\vec{K}), \quad (6)$$

where  $K_x$  ( $K_y$ ) is the momentum along (perpendicular) to the edge,  $t$  is the nearest neighbor inter-layer tunneling, and  $j$  denotes an internal flavor such as orbital index. In the presence of an internal symmetry, the chiral metal can undergo a phase transition associated with a spontaneous breaking of the symmetry, and a chiral non-Fermi liquid arises at the quantum critical point[22]. The full low-energy theory is decomposed into a set of decoupled patch theories. Each patch theory describes excitations near a set of points on the Fermi surface with a common tangent vector. For

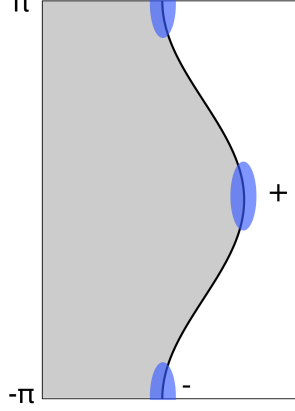


FIG. 2: A two-dimensional chiral Fermi surface realized on the surface of a stack of quantum Hall layers. Generically, there are two points on the Fermi surface which have a common tangent vector. For example, the points + and - have the same tangent vectors and they remain strongly coupled to each other in the low energy limit.

the dispersion in Eq. (6), there are generically two points with a parallel Fermi velocity as is shown in Fig. 2. The theory that includes the patches centered at  $\vec{K}_{F+} = (t, 0)$  and  $\vec{K}_{F-} = (-t, \pi)$  can be written as

$$\begin{aligned}
S = & \int \frac{d^3 \vec{k}}{(2\pi)^3} (i\eta k_0 + k_x + k_y^2) \psi_{js}^*(k) \psi_{js}(k) \\
& + \frac{1}{2} \int \frac{d^3 q}{(2\pi)^3} q_y^2 |\phi_\alpha(q)|^2 \\
& + g \int \frac{d^3 k d^3 q}{(2\pi)^6} \phi_\alpha(q) \psi_{is}^*(k+q) T_{is;jt}^\alpha \psi_{jt}(k).
\end{aligned} \tag{7}$$

Here  $\psi_{js}(k)$  is a chiral fermionic field with patch  $s = \pm$  which are related to the microscopic fermion field through  $\psi_{j+}(k_0, \vec{k}) = c_j(k_0, \vec{K}_{F+} + \vec{k})$ ,  $\psi_{j-}(k_0, \vec{k}) = c_j^*(-k_0, \vec{K}_{F-} - \vec{k})$ .  $\eta$  is a parameter that is introduced for a reason that will become clear soon.  $T_{is;jt}^\alpha$  is a matrix that describes the quantum number of the order parameter. For the SU(2) internal symmetry,  $T_{i+;j+}^\alpha = \tau_{ij}^\alpha$ ,  $T_{i-;j-}^\alpha = -(\tau^\alpha)_{ij}^T$  and  $T_{i+;j-}^\alpha = T_{i-;j+}^\alpha = 0$ , where  $\tau^\alpha$  are the generators of SU(2) group with  $\alpha = 1, 2, 3$ .

In two dimensions, the conventional perturbative expansion becomes unreliable as the coupling becomes large at low energies. Since the interaction plays a dominant role, we need to include the interaction up front rather than treating it as a perturbation to the kinetic energy. Therefore, we consider an interaction-driven scaling in which the fermion-boson coupling is deemed marginal. Under such a scaling, not all kinetic terms can be included as marginal operators. At the one-loop

order, the fermion self-energy is given by  $i|k_0|^{2/3}\text{sign}(k_0)$ , which suggests that the  $k_0$ -linear term should be irrelevant. The rest of the action is marginal if the dynamical critical exponent  $z \equiv [k_0]$  and the dimensions of the fields are chosen to be

$$z = \frac{3}{2}, \quad [\psi] = [\phi] = -2, \quad (8)$$

with  $[k_y] = 1/2$  with  $[k_x] = 1$ . The scaling dimension of  $k_y$  relative to  $k_x$  is fixed by the sliding symmetry.

Under the interaction-driven scaling,  $\eta$  has scaling dimension  $-1/2$ , and  $\eta^{-2}$  plays the role of a UV cut-off which is the only scale in Eq. (7). Since  $\eta$  is irrelevant by power counting, it is tempting to take the  $\eta \rightarrow 0$  limit, which is equivalent to taking the UV cut-off to infinity. In the small  $\eta$  limit, the theory has no scale. However, this alone neither guarantees the scale invariance of the theory nor protects the scaling dimensions in Eq. (8) from corrections even if the theory remains scale invariant. This is because of the scale anomaly. Even though the classical action has no scale, the quantum theory may not be well-defined without a UV cut-off. If so,  $\eta$  enters as a scale in the theory. The scale can in principle generate a gap, or modify the scaling dimensions in case the theory stays critical.

In the present theory, it turns out that  $\eta \rightarrow 0$  limit is well defined even at the quantum level due to chirality. First, the theory can not be gapped out because the chiral gapless modes are protected by the non-trivial topology (Chern number) in the bulk. Second, the theory remains finite in the  $\eta \rightarrow 0$  limit because quantum fluctuations that involve particle-hole excitations have limited phase space due to the chiral nature of the theory. In particular, all internal frequencies in loops are bounded by external frequencies, and loop integrations are finite in the small  $\eta$  limit due to a holomorphic structure inherited from the chirality[22]. This is analogous to the chiral Luttinger liquid in one dimension[46]. As a result, the theory remains critical, and the quantum theory has no scale. This implies that the scaling dimensions in Eq. (8) are exact. The full fermion Green's function obeys the scaling form,

$$G(k) = \frac{1}{\delta_k} g\left(\frac{k_0^{2/3}}{\delta_k}\right), \quad (9)$$

where  $\delta_k = k_x + k_y^2$ . The universal function  $g(x)$  is not fixed by the scaling, and the exact form of  $g(x)$  can, in principle, be very different from what is inferred from the one-loop Green's function. Nonetheless, the exponent is protected from quantum corrections. This is a stable non-Fermi liquid, which exhibits chaotic dynamics[47].

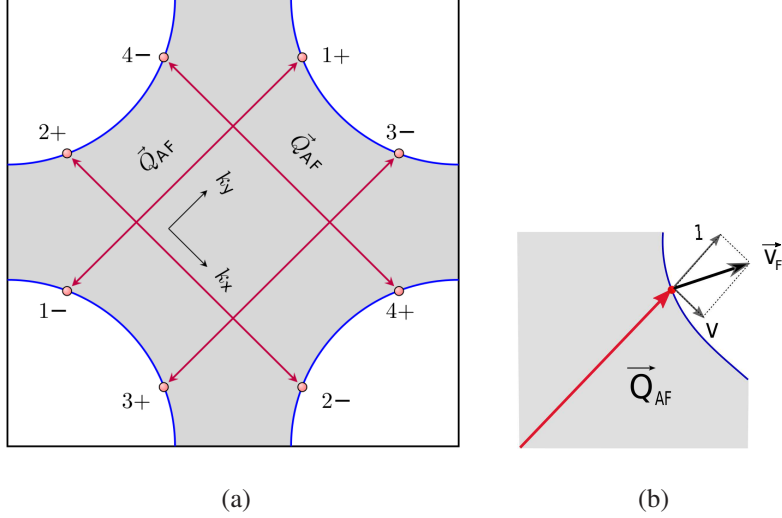


FIG. 3: (a) Eight hot spots connected by the antiferromagnetic ordering vector  $\vec{Q}_{AF}$  on a two-dimensional Fermi surface with  $C_4$  symmetry. (b) Decomposition of the Fermi velocity at hot spot 1+ into the component parallel to  $\vec{Q}_{AF}$  and the component perpendicular to  $\vec{Q}_{AF}$ . By rescaling momentum, the component parallel to  $\vec{Q}_{AF}$  is set to be one. The component perpendicular to  $\vec{Q}_{AF}$  denoted as  $v$  measures the degree of local nesting between the hot spots connected by  $\vec{Q}_{AF}$ .

### III. THEORY OF HOT SPOTS

In this section, we turn to the second type of non-Fermi liquids, where only a part of Fermi surface remains strongly coupled with a gapless collective mode. To be concrete, we consider the non-Fermi liquid realized at the  $SU(2)$  symmetric antiferromagnetic (AF) quantum critical point with a commensurate wave vector in two dimensions. With the  $C_4$  symmetry, the low-energy degrees of freedom consist of the AF collective mode coupled to electrons near eight hot spots, which are the points on the Fermi surface connected by the AF ordering vector [37, 48–50], as is shown in Fig. 3(a). The minimal model is written as

$$\begin{aligned}
\mathcal{S} = & \sum_{n=1}^4 \sum_{m=\pm} \sum_{\sigma=\uparrow,\downarrow} \int \frac{d^3k}{(2\pi)^3} \psi_{n,\sigma}^{(m)*}(k) \left[ ik_0 + e_n^m(\vec{k}; v) \right] \psi_{n,\sigma}^{(m)}(k) \\
& + \frac{1}{2} \int \frac{d^3q}{(2\pi)^3} [q_0^2 + c^2|\vec{q}|^2] \vec{\phi}(-q) \cdot \vec{\phi}(q) \\
& + g_0 \sum_{n=1}^4 \sum_{\sigma,\sigma'=\uparrow,\downarrow} \int \frac{d^3k}{(2\pi)^3} \frac{d^3q}{(2\pi)^3} \left[ \vec{\phi}(q) \cdot \psi_{n,\sigma}^{(+)*}(k+q) \vec{\tau}_{\sigma,\sigma'} \psi_{n,\sigma'}^{(-)}(k) + c.c. \right]
\end{aligned}$$

$$+u_0 \int \frac{d^3k}{(2\pi)^3} \frac{d^3p}{(2\pi)^3} \frac{d^3q}{(2\pi)^3} \left[ \vec{\phi}(k+q) \cdot \vec{\phi}(p-q) \right] \left[ \vec{\phi}(-k) \cdot \vec{\phi}(-p) \right]. \quad (10)$$

Here,  $k = (k_0, \vec{k})$  denotes the Matsubara frequency and the two-dimensional momentum  $\vec{k} = (k_x, k_y)$ .  $\psi_{n,\sigma}^{(m)}$  are the fermion fields that carry spin  $\sigma = \uparrow, \downarrow$  at the hot spots labeled by  $n = 1, 2, 3, 4$ ,  $m = \pm$ . The coordinate axes have been chosen such that the ordering wave vector is  $\vec{Q}_{AF} = \pm\sqrt{2}\pi\hat{k}_x, \pm\sqrt{2}\pi\hat{k}_y$  up to the reciprocal lattice vectors  $\sqrt{2}\pi(\hat{k}_x \pm \hat{k}_y)$ . With this choice the fermion dispersions are  $e_1^\pm(\vec{k}; v) = -e_3^\pm(\vec{k}; v) = vk_x \pm k_y$ ,  $e_2^\pm(\vec{k}; v) = -e_4^\pm(\vec{k}; v) = \mp k_x + vk_y$ , where  $\vec{k}$  is the momentum deviation from each hot spot. The Fermi velocity along the ordering vector has been set to be one by rescaling  $\vec{k}$ .  $v$  is the component of Fermi velocity that is perpendicular to  $\vec{Q}_{AF}$  as is shown in Fig. 3(b). The curvature of the Fermi surface can be ignored, since the patches of Fermi surface connected by the ordering vector are not parallel to each other with  $v \neq 0$ .  $\vec{\phi}(q)$  is the boson field with three components of the AF collective mode with frequency  $q_0$  and momentum  $\vec{Q}_{AF} + \vec{q}$ .  $\vec{\tau}$  represents the three generators of the  $SU(2)$  group.  $c$  is the velocity of the AF collective mode.  $g_0$  is the Yukawa coupling between the collective mode and the electrons near the hot spots, and  $u_0$  is the quartic coupling between the collective modes.

### A. Perturbative approach

In order to access the interacting non-Fermi liquid perturbatively, we deform the theory by tuning the number of co-dimensions of the Fermi surface[21, 37]. Since the the curvature near the hot spots can be ignored, the opposite sides of the Fermi surface are locally nested with a translation by momentum  $2\vec{K}_F$ . This allows us to pair fermions on opposite sides of the Fermi surface into two component spinors,  $\Psi_{1,\sigma} = (\psi_{1,\sigma}^{(+)}, \psi_{3,\sigma}^{(+)})^T$ ,  $\Psi_{2,\sigma} = (\psi_{2,\sigma}^{(+)}, \psi_{4,\sigma}^{(+)})^T$ ,  $\Psi_{3,\sigma} = (\psi_{1,\sigma}^{(-)}, -\psi_{3,\sigma}^{(-)})^T$ ,  $\Psi_{4,\sigma} = (\psi_{2,\sigma}^{(-)}, -\psi_{4,\sigma}^{(-)})^T$  to cast the fermionic action of Eq. (10) to the spinor form,  $S_F = \sum_{n=1}^4 \sum_{\sigma=\uparrow,\downarrow} \int \frac{d^3k}{(2\pi)^3} \bar{\Psi}_{n,\sigma}(k) \left[ i\gamma_0 k_0 + i\gamma_1 \varepsilon_n(\vec{k}; v) \right] \Psi_{n,\sigma}(k)$ , where  $\gamma_0 = \sigma_y$  and  $\gamma_1 = \sigma_x$ ,  $\bar{\Psi}_{n,\sigma} = \Psi_{n,\sigma}^\dagger \gamma_0$  with  $\varepsilon_1(\vec{k}; v) = e_1^+(\vec{k}; v)$ ,  $\varepsilon_2(\vec{k}; v) = e_2^+(\vec{k}; v)$ ,  $\varepsilon_3(\vec{k}; v) = e_1^-(\vec{k}; v)$ ,  $\varepsilon_4(\vec{k}; v) = e_2^-(\vec{k}; v)$ . The spinor components are different from the ones used in section II B. For hot Fermi surfaces, the local curvature of Fermi surface is important, and the spinor is formed out of a particle and a hole to maintain the nesting in the dispersion of the two components in the spinor. The theory in general dimensions can be written similarly as in Eq. (2)[21, 37]. The upper critical dimension is three, and the perturbative non-Fermi liquid can be accessed for small  $\epsilon = (3 - d)$ . The upper critical dimension is different from the one for the Ising-nematic critical

metal because the local curvature of Fermi surface is unimportant in the present case.

The action in general  $d$  continuously interpolates the original AF critical metal in two dimensions to the AF critical semi-metal with line nodes in three dimensions. The off-diagonal element of the kinetic term in general dimensions corresponds to a  $p$ -wave charge density wave which gaps out the otherwise  $(d-1)$ -dimensional Fermi surface into the line node. Similar to the Ising-nematic case, this breaks some internal symmetry. The original theory in Eq. (10) has  $SU(2) \times U(1)^4$  internal symmetry, where  $SU(2)$  is the spin rotation, and the four  $U(1)$ 's refer to the separate conservations of electron numbers in the four pairs of hot spots connected by  $\vec{Q}_{AF}$ . On the other hand, the theory in  $d > 2$  has only  $SU(2) \times U(1)^2$  as the off-diagonal kinetic term breaks two  $U(1)$ 's. One can ask how serious the symmetry breaking is in interpolating the results obtained in  $d > 2$  to  $d = 2$ . It turns out that the theory in any  $2 \leq d < 3$  can be solved exactly using a non-perturbative method to be discussed in the next section[51]. The critical exponents obtained in general dimensions smoothly interpolate to the answer in  $d = 2$ [52].

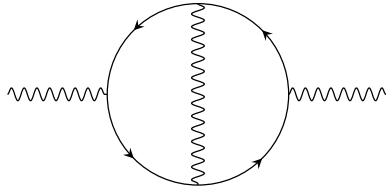


FIG. 4: Two-loop diagram that remains important even to the leading order in  $\epsilon$ . This diagram is nominally  $\epsilon^2$  but becomes enhanced to  $\epsilon$  due to the emergent quasilocality caused by the vanishing velocities.

A systematic perturbative analysis has been done for this model[37, 53] and a related model with the  $C_2$  symmetry[54]. Interestingly, all four parameters of the theory  $\{g, u, v, c\}$  flow to zero in the low energy limit. In particular, the Fermi surface near the hot spots exhibits an emergent nesting, and the collective mode slows down due to the Landau damping. Along with the emergent quasilocality, the couplings also flow to zero such that  $g^2/v \sim O(\epsilon)$ ,  $u/c^2 = 0$  at the fixed point. Unlike in relativistic field theories, it is not enough to consider only the one-loop graphs even to the leading order in  $\epsilon$ [37, 53, 54]. This is because the vanishingly small velocities can cause IR singularities at low energies such that some higher-loop corrections remain important even to the leading order in  $\epsilon$ . It turns out that in the small  $\epsilon$  limit one needs to include a two-loop graph shown in Fig. 4 in addition to the one-loop graphs. In the low energy limit, the coupling and the

velocities all flow to zero such that

$$\frac{g^2}{v} = 4\pi\epsilon, \quad \frac{g^2}{c^3} = \frac{1}{16\pi h_5^*}, \quad \frac{v}{c} = 0 \quad (11)$$

with  $h_5^* \approx 5.7 \times 10^{-4}$ . The two-loop diagram which is nominally order of  $\epsilon^2$  becomes enhanced to the order of  $\epsilon$  due to the quasilocality. Other higher-loop graphs remain small in the small  $\epsilon$  limit, and the  $\epsilon$ -expansion is controlled after the two-loop effect is included[53]. At the fixed point, the dynamical critical exponent and the scaling dimensions of the fundamental fields are given by

$$z = 1, \quad [\psi(k)] = -\frac{5 - \epsilon}{2}, \quad [\phi(k)] = -(3 - \epsilon). \quad (12)$$

It is noted that the fermion retains its classical dimension while the boson acquires a non-trivial anomalous dimension  $\eta_\phi = \epsilon/2$ . The boson is heavily dressed by particle-hole excitations, and it no longer propagates as a coherent excitation. On the other hand, the electrons remain largely intact in the low energy limit.

The most striking outcome revealed by the controlled expansion is the emergent hierarchy among three velocities : the component of the Fermi velocity along  $\vec{Q}_{AF}$  which is set to be one, the velocity of the collective mode ( $c$ ), and the component of the Fermi velocity perpendicular to  $\vec{Q}_{AF}$  ( $v$ ). In the low energy limit,  $c$  and  $v$  flow to zero such that  $v \ll c \ll 1$ . This poses both challenge and opportunity. On the one hand, higher-loop diagrams are not trivially suppressed even to the leading order in  $\epsilon$  due to the infrared singularity caused by the emergent locality. On the other hand, the ratios among velocities can be used as small parameters to solve the strongly interacting theory even in two dimensions[55].

## B. Non-perturbative approach

In order to tackle the theory in two dimensions directly, we start with an interaction-driven scaling that incorporates the interaction up front. Once the fermion-boson coupling is deemed marginal, one cannot keep all the kinetic terms as marginal operators. In choosing the marginal terms in the kinetic energy, we make a choice different from II B. Here we choose a scaling in which all the fermion kinetic term is kept marginal at the expense of discarding the entire boson kinetic term as irrelevant terms. This choice is inspired from Eq. (12). The marginality of the fermion kinetic term and the fermion-boson coupling uniquely fixes the dynamical critical exponent and the scaling dimensions,

$$z = 1, \quad [\psi(k)] = [\phi(k)] = -2. \quad (13)$$

This Ansatz is obtained by setting  $\epsilon = 1$  in Eq. (12). In general, one would expect higher-order corrections in  $\epsilon$ . In the present case, it turns out that Eq. (13) becomes exact in the low-energy limit because of the emergent hierarchy among the velocities[52].

Under Eq. (13), the entire boson kinetic term and the quartic coupling are irrelevant. The minimal action which includes only marginal terms is written as

$$\begin{aligned} \mathcal{S} = & \sum_{n=1}^4 \sum_{\sigma=\uparrow,\downarrow} \int dk \bar{\Psi}_{n,\sigma}(k) \left[ i\gamma_0 k_0 + i\gamma_1 \varepsilon_n(\vec{k}) \right] \Psi_{n,\sigma}(k) \\ & + i\sqrt{\frac{\pi v}{2}} \sum_{n=1}^4 \sum_{\sigma,\sigma'} \int dk dq \bar{\Psi}_{\bar{n},\sigma}(k+q) \vec{\tau}_{\sigma,\sigma'} \gamma_1 \Psi_{n,\sigma'}(k) \cdot \vec{\phi}(q). \end{aligned} \quad (14)$$

Here, we rescale the boson field to set the fermion-boson coupling to be proportional to  $\sqrt{v}$ . This is a convenient choice because the interaction is screened such that  $g^2$  becomes  $O(v)$  in the low-energy limit[37]. Although one can tune  $g$  and  $v$  independently in a microscopic theory, they flow to a universal line defined by  $g^2 \sim v$  at low energies[53].

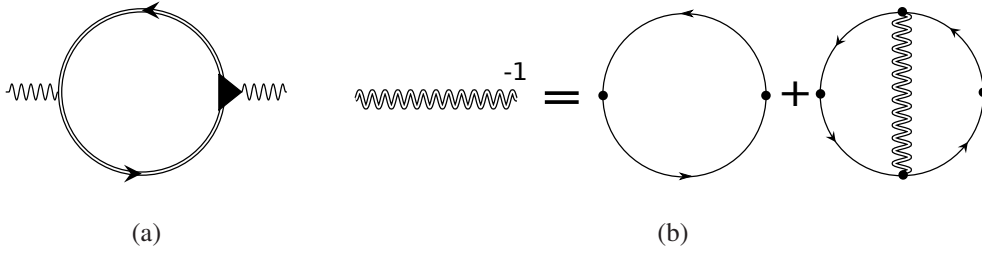


FIG. 5: (a) The exact boson self-energy. The double line is the fully dressed fermion propagator. The triangle represents the fully dressed vertex. (b) The reduced Schwinger-Dyson equation that replaces (a) in the small  $v/c$  limit.

In the absence of the bare action for boson, dynamics for the collective mode is entirely generated from particle-hole excitations as is shown in Fig. 5(a). The exact Schwinger-Dyson equation for the boson propagator reads

$$D(q)^{-1} = m_{CT} - \pi v \sum_n \int dk \text{Tr} [\gamma_1 G_{\bar{n}}(k+q) \Gamma(k,q) G_n(k)]. \quad (15)$$

Here  $D(k)$ ,  $G(k)$  and  $\Gamma(k,q)$  represent the fully dressed propagators of the boson and the fermion, and the vertex function, respectively.  $m_{CT}$  is a mass counter term that is added to tune the renormalized mass to zero. The trace is over the spinor indices. An Ansatz for  $D(q)$  that is consistent with Eq. (13) is

$$D(q)^{-1} = |q_0| + c(v) \left[ |q_x| + |q_y| \right]. \quad (16)$$

One needs to show that Eq. (16) indeed satisfies the Schwinger-Dyson equation, and determine the ‘velocity’ of the strongly damped collective mode  $c(v)$  as a function of  $v$ . Although the Schwinger-Dyson equation cannot be solved in general, it can be solved in the limit  $v/c(v)$  is small. Given that we don’t know whether  $v/c(v)$  flows to zero in two dimensions yet, we first solve the Schwinger-Dyson equation under the assumption that  $v \ll c(v) \ll 1$ , and then prove that  $v$ ,  $c(v)$  and  $v/c(v)$  indeed flow to zero using the solution of the Schwinger-Dyson equation.

In the small  $v/c(v)$  limit, the Schwinger-Dyson equation can be simplified. In particular, the full fermion propagator and the vertex function in Eq. (15) can be replaced with the bare fermion propagator and the one-loop dressed vertex function respectively to the leading order in  $v/c(v)$ . This can be understood in the following way[53]. The interaction mixes the fermions in patches connected by  $\vec{Q}_{AF}$ . This renormalizes the velocity of fermions such that the Fermi surface becomes locally nested near the hot spots[37, 48, 50, 53, 56, 57]. A well-nested Fermi surface provides a large phase space for soft particle-hole excitations that screen the interaction to  $g^2 \sim v$ . The flat spectrum of the particle-hole excitations also slows down the collective mode. The slow velocity of the collective mode enhances the feedback of the collective mode to the fermion. However, it is not strong enough to overcome the suppression caused by large screening. This is because the velocity of the collective mode remains larger than  $v$  due to the anti-screening effect of the vertex correction in Fig. 4 that speeds up the collective mode[52, 54]. Therefore, the fermion self-energy and the vertex correction is suppressed by  $g^2/c(v) \sim v/c(v)$ . Although both fermion self-energy and vertex corrections are small in the small  $v/c(v)$  limit, the leading vertex correction needs to be kept in Eq. (15). This is because the one-loop boson self-energy with the bare vertex is independent of momentum. In order to keep the minimal momentum dependence in the boson propagator, the one-loop vertex correction should be included in the Schwinger-Dyson equation. Therefore, the full Dyson equation is reduced to Fig. 5(b) in the small  $v/c(v)$  limit.

The solution to the reduced Schwinger-Dyson equation is indeed given by Eq. (16) with

$$c(v) = \frac{1}{4} \sqrt{v \log(1/v)}, \quad (17)$$

and the hierarchy is satisfied,  $v \ll c(v) \ll 1$  in the small  $v$  limit. The remaining job is to show that  $v$  flows to zero. The RG flow of  $v$  is determined from the fermion self-energy and the vertex correction computed with the dressed boson propagator. Under the RG flow,  $v$  flows to zero with increasing logarithmic length scale  $l$  as

$$\frac{dv}{dl} = -\frac{6}{\pi^2} v^2 \log\left(\frac{1}{c(v)}\right). \quad (18)$$

This completes the cycle of self-consistency. Eq. (16) obtained in the small  $v$  limit becomes asymptotically exact in the low-energy limit within a nonzero basin of attraction in the space of  $v$  near  $v = 0$ . We emphasize that the theory is still strongly coupled in the small  $v$  limit in that the conventional perturbative expansion is controlled by  $g^2/v \sim 1$ . One manifestation of this is that Fig. 5(b) includes an infinite series of diagrams that are all same order of magnitude.

If the bare value of  $v$  is small, there exist well-separated energy scales which dictate multiple crossovers. The first crossover is set by the competition between Eq. (16) and the irrelevant local kinetic term  $\frac{|q|^2}{\tilde{\Lambda}}$ , where  $\tilde{\Lambda}$  represents an energy scale introduced by rescaling the boson field from Eq. (10). For  $\omega < E_b^*$  with  $E_b^* = c^2\tilde{\Lambda}$ , the terms linear in frequency and momentum dominate. The second energy scale is the superconducting transition temperature. The spin fluctuations renormalize pairing interactions near the hot spots, and enhance the  $d$ -wave superconductivity[58–63]. Due the gapless collective mode which mediates a marginal interaction, the pairing vertex at frequency  $\omega$  is enhanced by double logarithms,  $\alpha \frac{v}{c} \log \frac{\Lambda}{\omega} \log \frac{E_b^*}{\omega}$  with  $\alpha \sim 1$ [39, 64, 65]. This gives  $T_c \sim c\sqrt{\Lambda\tilde{\Lambda}}e^{-\frac{1}{2\sqrt{\alpha}}\frac{\log^{1/2}1/v}{v^{1/4}}}$ . The third energy scale, denoted as  $E_f^*$ , is the one below which the behavior of the fermions at the hot spots deviates from the Fermi liquid one. For a small  $v$ , the leading order self-energy correction to the fermion propagator is  $\frac{3}{4\pi}\frac{v}{c}\omega \log \frac{\Lambda}{\omega}$ , which becomes larger than the bare term for  $\omega < E_f^*$  with  $E_f^* \sim \Lambda e^{-\frac{\pi}{3}\sqrt{\frac{\log 1/v}{v}}}$ . This scale is small because the fermion is only weakly perturbed by the collective mode. Finally, the value of  $v$  changes appreciably below  $E_v^* \sim \Lambda e^{-\frac{1}{v \log 1/v}}$ , which is determined from Eq. (18).

In the small  $v$  limit, there is a hierarchy among the energy scales,  $E_v^* \ll E_f^* \ll T_c \ll E_b^*$ . This suggests that the system undergoes a superconducting transition before the fermions at the hot spots lose coherence or  $v$  changes appreciably. On the other hand, there is a large window between  $T_c$  and  $E_b^*$  within which the universal scaling for the collective mode given by Eq. (16) is obeyed. The size of the energy window for the critical scaling is non-universal due to the slow flow of  $v$ , and it depends on the bare value of  $v$ . It is expected that the energy window for the  $z = 1$  critical scaling above  $T_c$  is larger in materials whose bare Fermi surfaces are closer to perfect nesting near the hot spots.

#### IV. CONCLUSION

Low-energy effective theories for non-Fermi liquids have unusual features that originate from the presence of infinitely many gapless modes. Strong infrared quantum fluctuations modify the

way in which quantum corrections are organized compared to relativistic quantum field theories. Quantum corrections that are normally considered to be higher-order effects should be included to the leading order even near the upper critical dimensions. Interestingly, this strong quantum effect is responsible for a remarkable simplicity that emerges in the low energy limit. In particular, the interaction-driven scaling which takes into account interactions ahead of the kinetic term at the ‘tree’-level gives exact critical exponents in some strongly coupled non-Fermi liquids.

It appears that the solvability of the strongly coupled field theories is rooted to the fact that the interaction-driven scaling is as far as interactions can do in critical states. The low-energy scaling is the result of competition between the interactions that tend to pin particles in real space and the kinetic energy that promotes delocalization. When the kinetic energy dominates as in Fermi liquids, the interactions play only limited roles, and the scaling that prioritizes the kinetic energy emerges. If interactions are strong, one can have a localized state such as Mott insulators depending on the density of particles. However, if an insulating state is not an option for itinerant quantum critical points, the way particles propagate is conformed by the dominant interaction so that the bare kinetic term can be completely ignored, which gives rise to the interaction-driven scaling. It remains to be understood how large the class of strongly coupled theories that obey the same principle is. It will be also interesting to search for yet another simple dynamical principles that may open up new windows to non-perturbative physics of strongly interacting systems. On the phenomenological side, many open questions are waiting to be addressed. For example, non-equilibrium phenomena in general, and the interplay of non-Fermi liquid behavior with impurities are interesting open problems.

**Acknowledgment** The author thanks Denis Dalidovich, Peter Lunts, Ipsita Mandal, Andres Schliefl and Shouvik Sur, for collaborations on the subject. The research was supported by the Natural Sciences and Engineering Research Council of Canada. Research at the Perimeter Institute is supported in part by the Government of Canada through Industry Canada, and by the Province of Ontario through the Ministry of Research and Information.

---

[1] L. Landau, *Sov. Phys. JETP* **3**, 920 (1957).

[2] J. Polchinski, *ArXiv High Energy Physics - Theory e-prints* (1992), [hep-th/9210046](https://arxiv.org/abs/hep-th/9210046) .

[3] R. Shankar, *Rev. Mod. Phys.* **66**, 129 (1994).

- [4] J. A. Hertz, [Phys. Rev. B \*\*14\*\*, 1165 \(1976\)](#).
- [5] A. J. Millis, [Phys. Rev. B \*\*48\*\*, 7183 \(1993\)](#).
- [6] H. v. Löhneysen, A. Rosch, M. Vojta, and P. Wölfle, [Rev. Mod. Phys. \*\*79\*\*, 1015 \(2007\)](#).
- [7] G. R. Stewart, [Rev. Mod. Phys. \*\*73\*\*, 797 \(2001\)](#).
- [8] T. Senthil, [Phys. Rev. B \*\*78\*\*, 035103 \(2008\)](#).
- [9] T. Holstein, R. E. Norton, and P. Pincus, [Phys. Rev. B \*\*8\*\*, 2649 \(1973\)](#).
- [10] M. Y. Reizer, [Phys. Rev. B \*\*40\*\*, 11571 \(1989\)](#).
- [11] B. L. Altshuler, L. B. Ioffe, and A. J. Millis, [Phys. Rev. B \*\*50\*\*, 14048 \(1994\)](#).
- [12] Y. B. Kim, A. Furusaki, X.-G. Wen, and P. A. Lee, [Phys. Rev. B \*\*50\*\*, 17917 \(1994\)](#).
- [13] P. A. Lee, [Phys. Rev. Lett. \*\*63\*\*, 680 \(1989\)](#).
- [14] J. Polchinski, [Nuclear Physics B \*\*422\*\*, 617 \(1994\)](#).
- [15] P. A. Lee and N. Nagaosa, [Phys. Rev. B \*\*46\*\*, 5621 \(1992\)](#).
- [16] C. Nayak and F. Wilczek, [Nuclear Physics B \*\*417\*\*, 359 \(1994\)](#).
- [17] S.-S. Lee, [Phys. Rev. B \*\*80\*\*, 165102 \(2009\)](#).
- [18] M. A. Metlitski and S. Sachdev, [Phys. Rev. B \*\*82\*\*, 075127 \(2010\)](#).
- [19] D. F. Mross, J. McGreevy, H. Liu, and T. Senthil, [Phys. Rev. B \*\*82\*\*, 045121 \(2010\)](#).
- [20] H.-C. Jiang, M. S. Block, R. V. Mishmash, J. R. Garrison, D. Sheng, O. I. Motrunich, and M. P. Fisher, [Nature \*\*493\*\*, 39 \(2013\)](#).
- [21] D. Dalidovich and S.-S. Lee, [Phys. Rev. B \*\*88\*\*, 245106 \(2013\)](#).
- [22] S. Sur and S.-S. Lee, [Phys. Rev. B \*\*90\*\*, 045121 \(2014\)](#).
- [23] T. Holder and W. Metzner, [Phys. Rev. B \*\*92\*\*, 041112 \(2015\)](#).
- [24] V. Oganesyan, S. A. Kivelson, and E. Fradkin, [Phys. Rev. B \*\*64\*\*, 195109 \(2001\)](#).
- [25] W. Metzner, D. Rohe, and S. Andergassen, [Phys. Rev. Lett. \*\*91\*\*, 066402 \(2003\)](#).
- [26] M. J. Lawler and E. Fradkin, [Phys. Rev. B \*\*75\*\*, 033304 \(2007\)](#).
- [27] J. Rech, C. Pépin, and A. V. Chubukov, [Phys. Rev. B \*\*74\*\*, 195126 \(2006\)](#).
- [28] D. L. Maslov and A. V. Chubukov, [Phys. Rev. B \*\*81\*\*, 045110 \(2010\)](#).
- [29] M. Zacharias, P. Wölfle, and M. Garst, [Phys. Rev. B \*\*80\*\*, 165116 \(2009\)](#).
- [30] S.-S. Lee, [Phys. Rev. B \*\*78\*\*, 085129 \(2008\)](#).
- [31] P. Säterskog, B. Meszner, and K. Schalm, [ArXiv e-prints \(2016\), arXiv:1612.05326](#).
- [32] A. L. Fitzpatrick, S. Kachru, J. Kaplan, and S. Raghu, [Phys. Rev. B \*\*89\*\*, 165114 \(2014\)](#).
- [33] I. Mandal and S.-S. Lee, [Phys. Rev. B \*\*92\*\*, 035141 \(2015\)](#).

- [34] S. Chakravarty, R. E. Norton, and O. F. Syljuåsen, *Phys. Rev. Lett.* **74**, 1423 (1995).
- [35] A. L. Fitzpatrick, S. Kachru, J. Kaplan, and S. Raghuram, *Phys. Rev. B* **88**, 125116 (2013).
- [36] T. Senthil and R. Shankar, *Phys. Rev. Lett.* **102**, 046406 (2009).
- [37] S. Sur and S.-S. Lee, *Phys. Rev. B* **91**, 125136 (2015).
- [38] A. Eberlein, A. A. Patel, and S. Sachdev, *Phys. Rev. B* **95**, 075127 (2017).
- [39] D. T. Son, *Phys. Rev. D* **59**, 094019 (1999).
- [40] M. A. Metlitski, D. F. Mross, S. Sachdev, and T. Senthil, *Phys. Rev. B* **91**, 115111 (2015).
- [41] S. Raghuram, G. Torroba, and H. Wang, *Phys. Rev. B* **92**, 205104 (2015).
- [42] S. Lederer, Y. Schattner, E. Berg, and S. A. Kivelson, *Phys. Rev. Lett.* **114**, 097001 (2015).
- [43] I. Mandal, *Phys. Rev. B* **94**, 115138 (2016).
- [44] S. Lederer, Y. Schattner, E. Berg, and S. A. Kivelson, ArXiv e-prints (2016), [arXiv:1612.01542 \[cond-mat.str-el\]](https://arxiv.org/abs/1612.01542) .
- [45] L. Balents and M. P. A. Fisher, *Phys. Rev. Lett.* **76**, 2782 (1996).
- [46] X. G. Wen, *Phys. Rev. B* **41**, 12838 (1990).
- [47] A. A. Patel and S. Sachdev, *Proceedings of the National Academy of Sciences* **114**, 1844 (2017), <http://www.pnas.org/content/114/8/1844.full.pdf> .
- [48] A. Abanov and A. V. Chubukov, *Phys. Rev. Lett.* **84**, 5608 (2000).
- [49] A. Abanov and A. Chubukov, *Phys. Rev. Lett.* **93**, 255702 (2004).
- [50] M. A. Metlitski and S. Sachdev, *Phys. Rev. B* **82**, 075128 (2010).
- [51] A. Schliefer, P. Lunts, and S.-S. Lee, in preparation .
- [52] A. Schliefer, P. Lunts, and S.-S. Lee, ArXiv e-prints (2016), [arXiv:1608.06927 \[cond-mat.str-el\]](https://arxiv.org/abs/1608.06927) .
- [53] P. Lunts, A. Schliefer, and S.-S. Lee, ArXiv e-prints (2017), [arXiv:1701.08218 \[cond-mat.str-el\]](https://arxiv.org/abs/1701.08218) .
- [54] S. Sur and S.-S. Lee, *Phys. Rev. B* **94**, 195135 (2016).
- [55] Y. Huh and S. Sachdev, *Phys. Rev. B* **78**, 064512 (2008).
- [56] A. Abanov, A. V. Chubukov, and J. Schmalian, *Advances in Physics* **52**, 119 (2003), <http://www.tandfonline.com/doi/pdf/10.1080/0001873021000057123> .
- [57] S. A. Maier and P. Strack, *Phys. Rev. B* **93**, 165114 (2016).
- [58] D. Scalapino, E. Loh Jr, and J. Hirsch, *Physical Review B* **34**, 8190 (1986).
- [59] K. Miyake, S. Schmitt-Rink, and C. M. Varma, *Phys. Rev. B* **34**, 6554 (1986).
- [60] T. Moriya, Y. Takahashi, and K. Ueda, *Journal of the Physical Society of Japan* **59**, 2905 (1990), <http://dx.doi.org/10.1143/JPSJ.59.2905> .

- [61] E. Berg, M. A. Metlitski, and S. Sachdev, *Science* **338**, 1606 (2012), <http://www.sciencemag.org/content/338/6114/1606.full.pdf> .
- [62] Z.-X. Li, F. Wang, H. Yao, and D.-H. Lee, ArXiv e-prints (2015), [arXiv:1512.04541](https://arxiv.org/abs/1512.04541) [cond-mat.supr-con] .
- [63] Y. Schattner, M. H. Gerlach, S. Trebst, and E. Berg, *Phys. Rev. Lett.* **117**, 097002 (2016).
- [64] P. Monthoux, A. V. Balatsky, and D. Pines, *Phys. Rev. B* **46**, 14803 (1992).
- [65] A. V. Chubukov and J. Schmalian, *Phys. Rev. B* **72**, 174520 (2005).